RELAY-ASSISTED OFDM-BASED VISIBLE LIGHT COMMUNICATIONS

A Thesis

by

Ömer Narmanlıoğlu

Submitted to the
Graduate School of Sciences and Engineering
In Partial Fulfillment of the Requirements for
the Degree of

Master of Science

in the
Department of Electrical and Electronics Engineering

Özyeğin University
August 2016

RELAY-ASSISTED OFDM-BASED VISIBLE LIGHT COMMUNICATIONS

Approved by:

Prof. Dr. Murat Uysal, Advisor
Department of Electrical and Electronics Engineering
Özyeğin University

Asst. Prof. Cenk Demiroğlu
Department of Electrical and Electronics Engineering
Özyeğin University

Asst. Prof. Tuncer Baykaş
Department of Electrical and Electronics Engineering
İstanbul Medipol University

Date Approved: 5 August 2016

ABSTRACT

In this study, a relay-assisted visible light communication (VLC) system where an intermediate light source cooperates with the main light source is investigated. Specifically, two light sources in an office space; one is the information source employed on the ceiling and the other one is a task light, are considered. The system uses DC biased optical orthogonal frequency division multiplexing (DCO-OFDM) where the task light performs relaying to assist the communication and operates in half-duplex (HD) mode for both amplify-and-forward (AF) and decode-and-forward (DF) relaying. The bit error rate (BER) performance of the relay-assisted VLC system is investigated and the performance is further optimized through optimal AC/DC power allocation under illumination constraints. The DC power allocation is determined by sharing the number of light emitting diode (LED) chips between the terminals to satisfy a desired luminance ratio. The AC power allocation decides the fraction of the information signal power to be consumed at the terminals in order to minimize the BER. Numerical results reveal that cooperation brings significant performance gains over direct transmission.

ÖZETÇE

Bu çalışmada, röle destekli görünür ışık haberleşmesi (visible light communication, VLC) araştırıldı. Biri, ana kaynak olarak tanımlanan, aydınlatma ve bilgi iletimi amacıyla tavana yerleştirilen, diğeri ise röle olarak adlandırılan ve çalışma masası üzerinde yakından aydınlatma amacıyla bulunan, toplam iki tane ışık-yayan-diyot (light emitting diode, LED) içeren bir oda düşündüldü. Çalışma masası üzerindeki ışık kaynağı, tavandaki kaynaktan gelen bilgi sinyalini, yükselt-ve-ilet (amplify-and-forward, AF) ya da çöz-ve-ilet (decode-and-forward, DF) yöntemleriyle, işleyerek bilgi iletimin güçlenmesine yardımcı olur. Bu işlem, çift yönlü (half-duplex, HD) iletim modunda, doğru akım eklenen optik dikey frekans bölmeli çoklama (direct current biased optical orthogonal frequency division multiplexing, DCO-OFDM) tekniğini kullanarak çalışır. Bu tekniğin içerdiği DC güç, ışık seviyesini; AC güç ise bilgi sinyalinin gücünü belirler. Önerilen sistem modeli üzerinde, aydınlatma koşullarını dikkate alarak, bit-hata-oranı (bit-error-rate, BER) analizi ve ana kaynak/röle arasında AC/DC güç paylaşımı üzerinden iyileştirmesi yapıldı. Bu iyileştirme sırasında, öncelikle toplam DC gücü, aydınlatmayı istenen seviyeye getirmek için dağıtıp; AC güç ana kaynak ve röle arasında, sistemin performansını iyileştirmek için paylastırıldı. Direk (röle destekli olmayan) haberleşme performansının kıstas olarak alındığı sonuçlarda, önemli performans kazançları gözlendi.

ACKNOWLEDGEMENTS

I would like to thank my family for always supporting me as I have pursued my education.

TABLE OF CONTENTS

LIST OF TABLES

LIST OF FIGURES

CHAPTER I

INTRODUCTION

Visible light communication (VLC) has emerged as an alternative short-range wireless transmission technique using light emitting diode (LED) [1] that can be modulated at very high speeds which are not noticeable to the human eye and without effect on illumination level. It uses visible light spectrum which is in the wavelength range of $390 - 700$ nm that corresponds to a frequency band of $430 - 770$ THz (see Fig. 1).

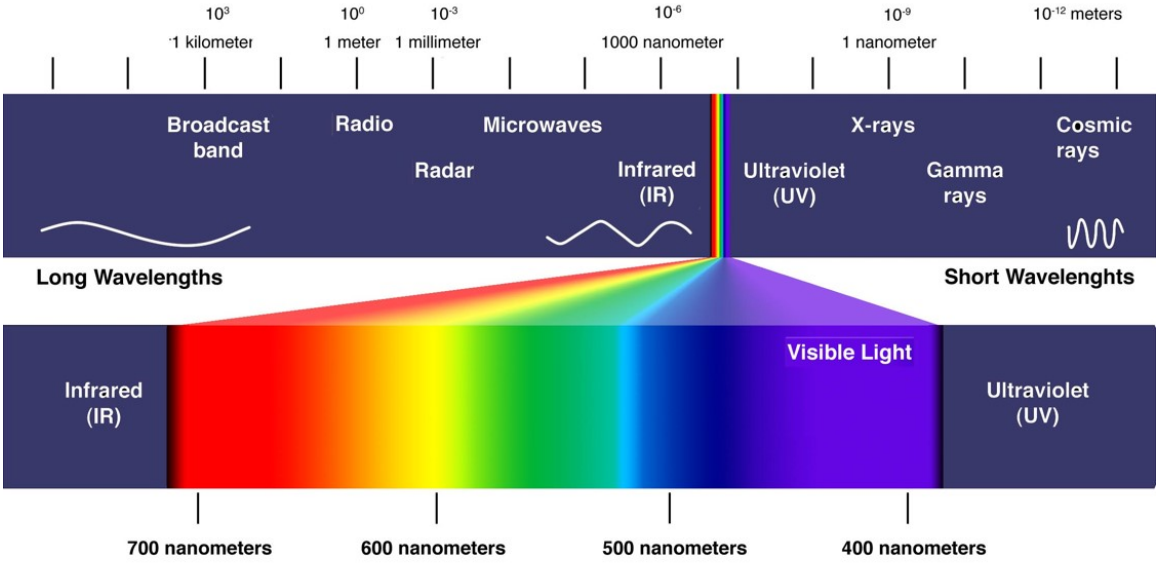

Figure 1: Visible light spectrum.

VLC provides a low-cost and energy-efficient solution since it is able to use the existing illumination infrastructure for data communication purposes. Therefore, this transmission technique also refers to the dual use of illumination infrastructure for wireless communications.

In VLC, intensity modulated and direct detection (IM/DD), where the signal driving the LEDs should be real valued and remain in the dynamic range of LEDs,

is used. Initial works on VLC use simple modulation techniques such as on-off keying (OOK) and pulse position modulation (PPM) [2]. Recent works have explored how multicarrier communications, particularly orthogonal frequency division multiplexing (OFDM) [3], can be used in the context of VLC. The VLC channel is of multipath nature and results in frequency-selectivity when high data speeds are targeted. An efficient approach to mitigate intersymbol interference (ISI) resulting from frequency-selectivity is OFDM. In OFDM, the high-rate data stream is demultiplexed and transmitted over a number of frequency subcarriers. OFDM has already been adopted in a number of radio frequency (RF) wireless standards such as digital broadcasting, cellular, and wireless local area networks. Such solutions, however, cannot be directly adopted for VLC systems. The design of optical OFDM (O-OFDM) requires certain modifications to take into account the non-negativity of the optical signal. This can be achieved by different methods including direct current biased OFDM (DCO-OFDM) [3], asymmetrically clipped O-OFDM (ACO-OFDM) [4] or flip-OFDM [5]. O-OFDM has been extensively investigated in the literature, see e.g., [6, 7, 8, 9, 10] and the references therein, but the current results are mainly limited to direct (point-to-point) transmission. In a typical indoor environment, there exists multiple light sources. In addition to ceiling luminaries, task lights (either desk lights or floor lights) are commonly used in office spaces and homes. Such secondary lights can be used as *relays*. In respect to them, this study investigates how cooperation between light sources can improve the error rate performance of an OFDM-based VLC system.

1.1 Related Works

Earlier works on relay assisted VLC systems include [11, 12, 13, 14, 15, 16, 17]. An LED-to-LED multi-hop LED system for toys is demonstrated in [11]. The work in [11] uses the reversed biased LED as a low-cost photodetector and targets very low

data rate applications, i.e., a few bits per second. In [12], a multi-user VLC system is proposed where the message is forwarded through other users (who act as relays) to the destination when the source-to-destination link is shadowed or blocked. Then, the performance of the multi-user system is evaluated in terms of medium access control (MAC) layer metrics such as collision rate and connectivity probability. In an experimental VLC study [13], an audio signal is successfully delivered to the destination over two intermediate relay terminals. In [14], a multi-hop inter-vehicular message forwarding scheme is considered for outdoor VLC systems and successful package delivery percentage is evaluated depending on the average inter-vehicle distance. In [15] and [16], a loop interference cancellation method is investigated for a full-duplex (FD) cooperative VLC system. The work in [17] investigates a scenario in which user terminals can act as relays in order to extend the coverage of VLC-based downlink.

1.2 Contributions

None of the above works on relay-assisted (cooperative) VLC systems are OFDM-based. Furthermore, they do not take into account the illumination constraints. In this work, an extensive performance evaluation and optimization of relay-assisted DCO-OFDM VLC systems under lighting constraints are presented. An office space where VLC is used for downlink wireless access is considered. It is assumed that the office has two light sources. One of them is placed at the ceiling to provide ambient light to the environment and the other one might be either a desk or floor light used for task lighting purposes. The task lights are commonly used in office spaces and they give each user the ability to control their own lighting, reduce the glare, and lower their eye strain [18]. It is assumed that the main ambient light source at the ceiling has direct access to the backbone network [2] from which data is fed to the source. The task light acts as a relay and assists the source to forward its data to the end user. Both amplify-and-forward (AF) and decode-and-forward (DF) relaying are

considered in the study. The main contributions of the study are as follows:

- In this work, a relay-assisted DCO-OFDM VLC system is considered and its performance through the derivation of signal-to-noise ratio (SNR) and bit error rate (BER) is investigated. The results demonstrate that relay-assisted transmission achieves performance gains over direct transmission. The level of gains are dependent on modulation type and topology.

- The system performance is further optimized under lighting constraints where two optimization parameters, K_L and K_E, are defined. The first parameter K_L controls the fraction of the total number of LED chips (which is directly related to the consumed DC power) shared between the source and relay terminals. The other parameter K_E controls the fraction of the total electrical information power (i.e., AC power) to be shared between the terminals. For task lighting, European Standard EN $12464-1$ recommends that the luminance ratio of the task surface to the adjacent walls should be less than 5 [19]. In the work, first K_L is determined to satisfy the recommended luminance ratio and then K_E is optimized to minimize the BER.

- Performance comparisons of AF and DF relaying are provided in the context of VLC and it is demonstrated that DF relaying provides higher BER performance gains over AF under the same lighting requirements.

- The dynamic range constraints of the LEDs are taken into account and the effect of clipping distortion on the BER performance of the relay-assisted DCO-OFDM VLC system under consideration is investigated.

CHAPTER II

INDOOR VLC CHANNEL MODEL

A typical office space with two different scenarios as in Fig. 2 is considered. In both scenarios, there are two light sources: one at the ceiling provides ambient light and the second is for task lighting. In addition to their lighting operation, the light source at the ceiling is considered as the main information source (S) and the task light is considered as the relay terminal (R). In the first scenario, the use of a desk light as the task light (see Fig. 2 (a)) is considered while a floor light is used in the second scenario (see Fig. 2 (b)).

The destination (D) terminal in the form of a Universal Serial Bus (USB) receiver which is located next to the computer on the desk is envisioned. When the center of the floor is set at $(0, 0, 0)$, the locations of the source and destination terminals are $(0, 0, 3)$ and $(1.6, 1.6, 0.7)$, respectively. The desk height is 70 cm. For each scenario, it is assumed that the height of task light is adjustable. The heights of desk light are 40 cm, 60 cm and 80 cm and the heights of floor light are 150 cm, 160 cm and 170 cm. Therefore, there is a total of 6 configurations as summarized in Table 1.

Table 1: Configurations under consideration.

Configuration	Relay Location	Type of Relay	Height of Relay
A	$(1.6, 1.6, 1.1)$	Desk light	40 cm
B	$(1.6, 1.6, 1.3)$	Desk light	60 cm
C	$(1.6, 1.6, 1.5)$	Desk light	80 cm
D	$(1.85, 1.85, 1.5)$	Floor light	150 cm
E	$(1.85, 1.85, 1.6)$	Floor light	160 cm
F	$(1.85, 1.85, 1.7)$	Floor light	170 cm

Reflection coefficients of the walls, ceiling, floor and desk surface are set at 0.8, 0.8, 0.3 and 0.8, respectively [18, 20]. For furniture items, i.e., chair, computer, the

reflection coefficient is taken as 0.37 [21] assuming that they are both black colored.

The following analysis discusses the illumination performance of the system and presents the power delay profiles for source-to-relay (S→R), source-to-destination (S→D), and relay-to-destination (R→D) links.

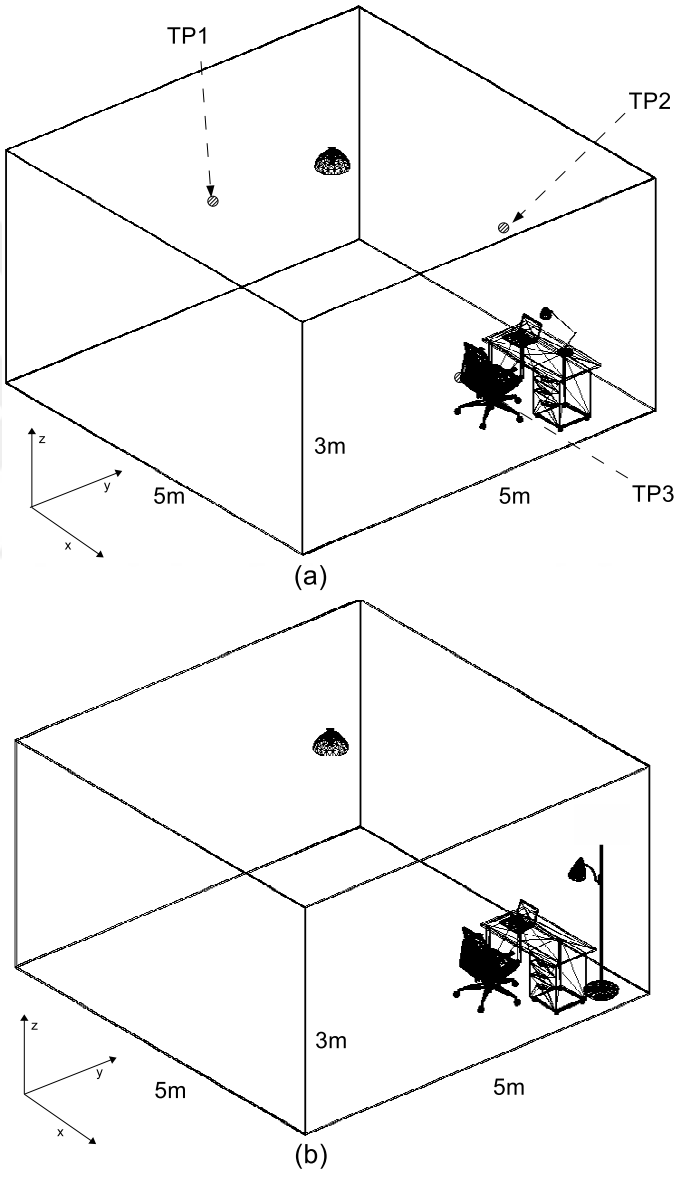

Figure 2: Physical room model (a) with desk light (b) with floor light.

2.1 Illumination Constraints

The emitted optical powers from the source and relay terminals affect both the communication and lighting performance (luminance) of the cooperative system. For a Lambertian surface, the luminance L (cd/m^2) is calculated as $L = \epsilon\rho/\pi$ where ρ is the reflectivity index and ϵ is the illuminance (defined as luminous flux per unit area [22] and measured in lux) on the surface. The horizontal and vertical illuminance are

$$\epsilon^h = \frac{I(0)\cos^m(\theta)\cos(\varphi)}{d^2} \tag{1}$$

$$\epsilon^v = \frac{I(0)\cos^m(\theta)\sin(\varphi)}{d^2} \tag{2}$$

where $I(0)$ is the center luminous intensity (cd), θ is the angle of irradiance, φ is the angle of incidence, d is the distance between the light source and the surface, and m is the Lambertian index.

In an office space, it is recommended that the luminance ratio of the task surface to the adjacent walls within the field of vision should be less than 5 [19]. In order to assess the luminance ratio in the proposed scenario, three test points (TPs) on the surrounding walls (see Fig. 2.a) are considered. The locations of the TP1, TP2 and TP3 are set at $(-2.5, 0, 1.5)$, $(0, 2.5, 1.5)$ and $(2.5, 0, 1.5)$, respectively. The illuminance levels on the desktop and the walls are obtained using (1) and (2), respectively. The luminances of the surfaces are then calculated and the luminance ratios of the desk surface to each adjacent wall are obtained. As an example, Fig. 3 presents the luminance ratios for Configuration A different values of K_L (under the assumption of that the total number of available LED chips is L_T; the source terminal employs $L_T K_L$ chips and the relay terminal employs $L_T(1 - K_L)$ chips) which denotes the fraction of the total number of LED chips at source and relay terminals. The Lambertian index m is set at 1.56. In Fig. 3, it is observed that for $K_L > 0.92$, the desired luminance ratio of less than 5 is achieved for Configuration A.

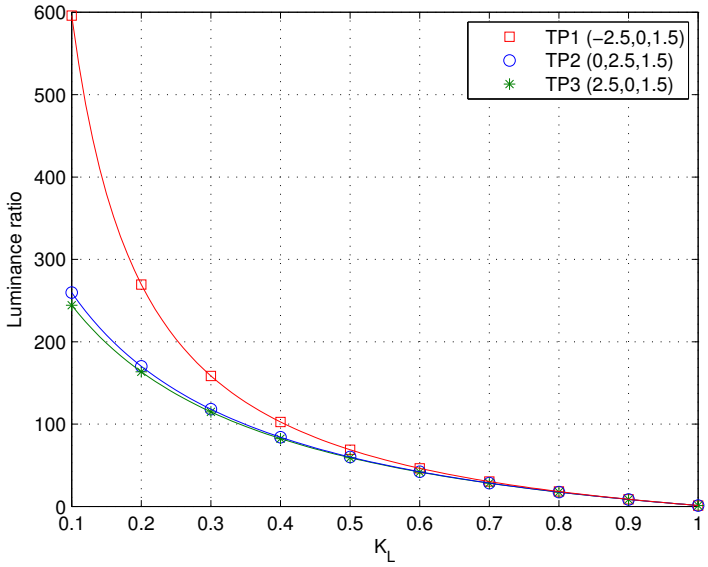

Figure 3: Luminance ratio between the task surface and the test points versus K_L for Configuration A.

2.2 Power Delay Profiles

The approach described in [23] and [24] is used for the channel modeling. First, a three dimensional model of the office space is created using Zemax® that integrates the two lighting sources (i.e., ceiling and task light) and photodetectors in the model. The areas of detectors at both the relay and destination terminals are taken as 1 cm^2 and the field-of-view (FOV) are set to 85°. It is assumed that the photodetector of the relay is placed at the top of the task light and directed towards the source. Whereas, the LEDs of the relay are at the bottom of the task light tilted to the desk surface. The luminaries are assumed to have Lambertian emission pattern. Using the non-sequential ray tracing features of Zemax®, the received optical power and the delays of direct/indirect rays and corresponding delays are calculated. This information is then imported into Matlab® and the corresponding Power Delay Profile (PDP) is obtained through proper normalizations. Fig. 4 illustrates the PDPs $c_{sd}(t)$, $c_{rd}(t)$ and $c_{sr}(t)$, respectively, for S→D, R→D, and S→R links for the six configurations under consideration.

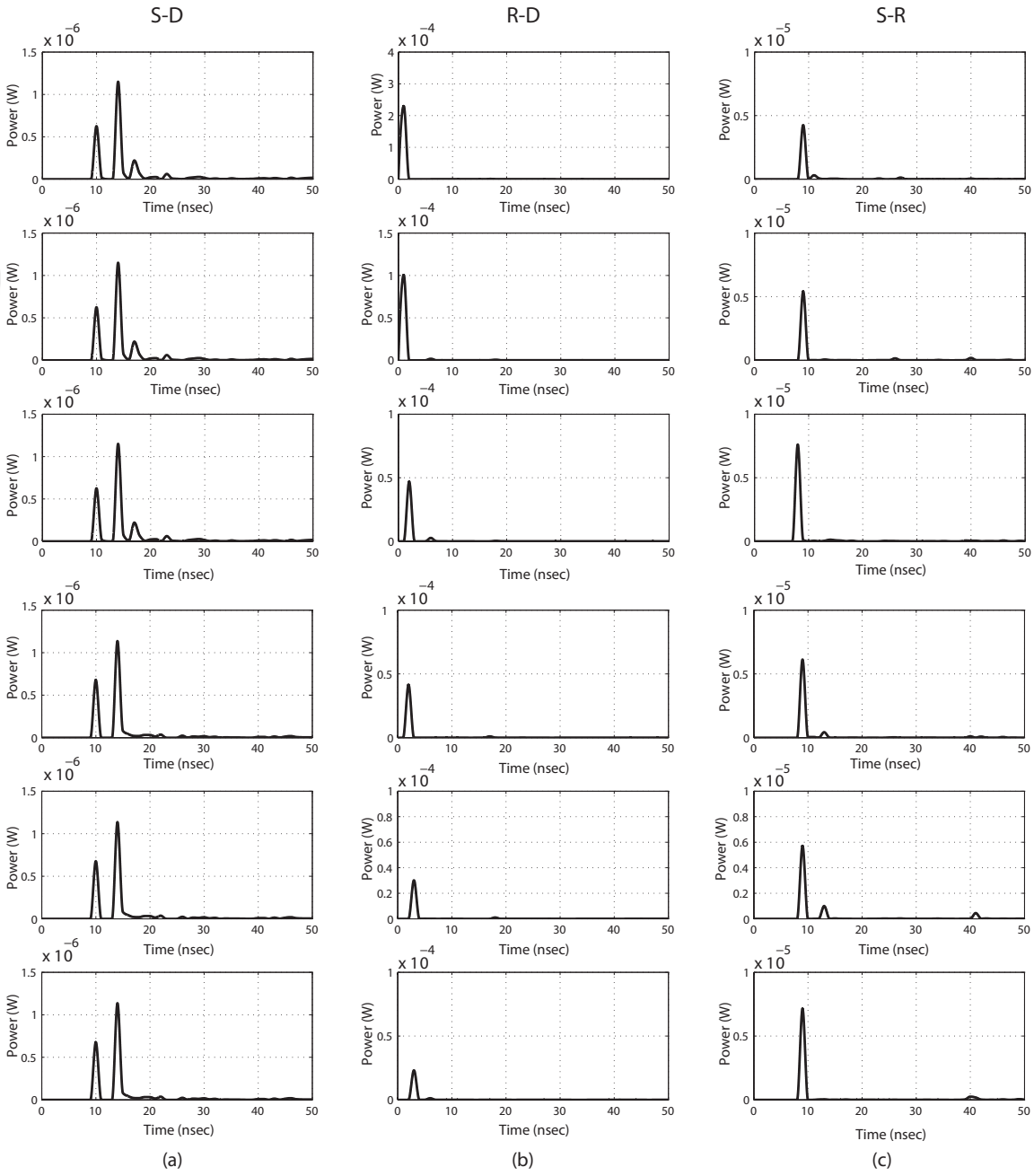

Figure 4: The PDPs for (a) S→D link, (b) R→D link and (c) S→R link.

CHAPTER III

SYSTEM MODEL

This chapter first provides the non-cooperative system model which will be used as a benchmark and then introduces details on the proposed relay-assisted system.

3.1 Non-Cooperative (Direct) Transmission

The block diagram of an O-OFDM VLC system without any intermediate terminal is given in Fig. 5.

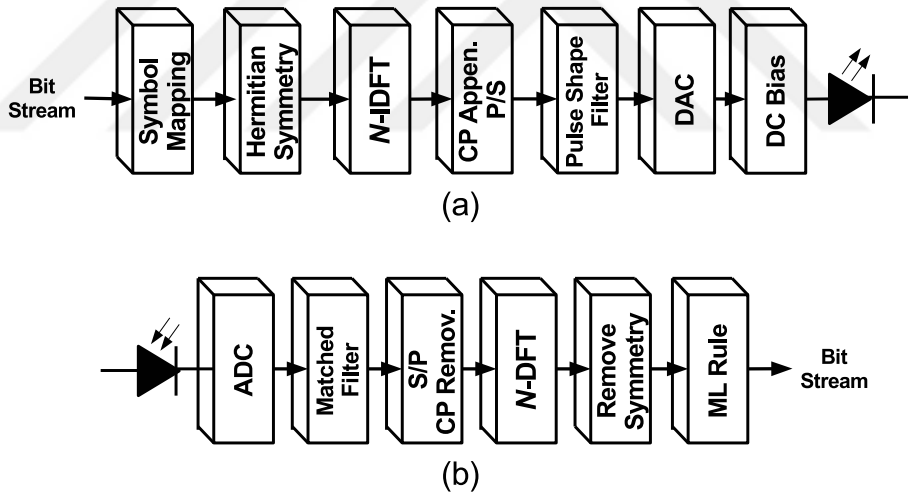

Figure 5: Block diagram of DCO-OFDM (a) transmitter and (b) receiver.

The input bit stream is first mapped to the complex symbols according to the deployed modulation scheme such as phase shift keying (PSK) or quadrature amplitude modulation (QAM). The input vector frame $\mathbf{X}$ is then passed through the N-inverse fast Fourier transform (IFFT) block to form the discrete waveform $x[n]$. One important constraint in IM/DD optical communication is that the information waveform $x[n]$ should be both real and non-negative. The electrical OFDM signal,

however, is both complex and bipolar. It is known that when the complex symbol vector $\mathbf{X}$ satisfies Hermitian symmetry, the IFFT output waveform $\mathbf{x}$ becomes real. The Hermitian symmetry can be reached by setting the input vector $\mathbf{X}$ such that $X[k] = X[N-k]^*$ for $0 < k < N/2$. $X[0]$ and $X[N/2]$ are also set to zero to prevent any DC shift at the output of IFFT. Therefore, the frame $\mathbf{X}$ has the form of

$$\mathbf{X} = [0 \quad s_1 \quad s_2 \quad ... \quad s_{N/2-1} \quad 0 \quad s^*_{N/2-1} \quad ... \quad s^*_2 \quad s^*_1]. \tag{3}$$

where $(.)^*$ is the complex conjugation. The output of the IFFT block is the time vector to be emitted by LEDs and can be obtained as

$$x[n] = \frac{1}{\sqrt{N}} \sum_{k=0}^{N-1} X[k] e^{j\frac{2\pi nk}{N}}. \tag{4}$$

A cyclic prefix (CP) with a length of N_g is then appended at the beginning of $x[n]$ to avoid intersymbol interference. The real-valued OFDM waveform $x(t)$ is written as

$$x(t) = \sum_{n=0}^{P-1} x[n]\delta(t - nT_s) \tag{5}$$

where $\delta(t)$ is the impulse function, T_s is the sampling interval, and $P = N + N_g$ is the total length of the OFDM symbol with appended cyclic prefix.

In DCO-OFDM, all the amplitude levels of the intensity waveform should be non-negative, therefore a bias voltage B should be added to (5). The DC bias voltage has direct impact on the clipping distortion. For example, in [9], optimum DC biasing is discussed for non-cooperative DCO-OFDM systems and it is shown that setting the DC bias to the middle of the dynamic range gives performance very close to that of optimum solution unless the dynamic range is wide.

Assume that V_{tov} is the turn-on voltage and V_{max} is the maximum allowed forward voltage. The amplitude levels of $x(t)$ beyond the dynamic range of the LED defined by [V_{tov},V_{max}] are clipped. The effect of clipping distortion will later be discussed in Chapter V and for now it is assumed that amplitude levels of $x(t)$ remain within the

dynamic range. The output of OFDM modulator therefore is simply given by $\overline{x}(t) = x(t)$.

In direct (non-cooperative) transmission, there is only the S→D link with no intermediate relay terminal. As defined earlier, L_T denotes the total number of available LED chips and in a direct transmission system all of them are used at the source terminal located at the ceiling. All of the LED chips are biased with the same DC value. The received electrical signal at the destination is therefore given by

$$y(t) = rg \sum_{i=1}^{L_T} x(t) \otimes h_{sd}(t) + v(t) \tag{6}$$

where $\otimes$ is the convolution operator, r is the responsivity of the photodetector (A/W), g is the gain of an LED (W/A), and $v(t)$ is the additive white Gaussian noise (AWGN) term with zero mean and variance of σ_n^2 (N(0,σ_n^2)) which includes the effects of thermal noise and the shot noise due to the ambient light. Without losing generality, $rg = 1$ is assumed for simplicity of the presentation. In (6), $h_{sd}(t)$ is the electrical channel impulse response (CIR) for the S→D link and is defined as $h_{sd}(t) = p(t) \otimes c_{sd}(t) \otimes p(-t)$ where $p(t)$ denotes the transmit pulse shaping filter response.

In frequency domain, the channel gain per subcarrier $H_{sd}[k]$ can be written as

$$H_{sd}[k] = \sum_{n=0}^{N_g} h_{sd}[n] e^{-j\frac{2\pi nk}{N}}. \tag{7}$$

where $h_{sd}[n] = h_{sd}(nTs)$. After taking the fast Fourier transform (FFT) of $y(nT_s)$ at the receiver, the received symbols are expressed as

$$Y[k] = L_T X[k] H_{sd}[k] + W[k]. \tag{8}$$

The destination then performs maximum likelihood decoding in order to recover the signals. If the energy of the channel $h_{sd}[n]$ is normalized to one, i.e., $\sum_{n=-\infty}^{+\infty} |h_{sd}[n]|^2 = 1$ and the energy of $x(t)$ is scaled to E, the average electrical SNR per subcarrier becomes, assuming unit time duration, $\gamma = L_T^2 E/\sigma_n^2$.

3.2 Relay Assisted Transmission

Consider the three-node dual-hop communication scenario where the source terminal (i.e., light source at the ceiling) communicates with the destination though a relay terminal (i.e., task light). In this relay-assisted transmission scenario, the relay terminal has no access to the backbone network and simply receives the information from the source and forwards it to the destination using the half-duplex (HD) orthogonal cooperation protocol of [25]. In the broadcasting phase, the source terminal transmits the information to both the relay and destination terminals. In the relaying phase, the source terminal remains silent and the relay terminal forwards the broadcasted message to the destination terminal.

The available OFDM signal energy used in the two cooperation phases (time slots) is set to $2E$ yielding an average power in proportion to E per time slot (assuming unit time duration). Optimization parameter K_E controls the fraction of the total information power $2E$ to be shared between the terminals. Specifically, each LED chip at the source and relay terminals will be allocated signal powers $2EK_E$ and $2E(1-K_E)$, respectively. The other optimization parameter K_L controls the fraction of the total number of LED chips to be shared between the source and relay terminals. It is assumed that all the LED chips at the source and relay terminals are biased with the same DC value.

In order to incorporate the effects of relay location, relative gains G_{sr} and G_{rd} for the S→R and R→D links, respectively, are considered. The relative gains can be calculated from $G_{sr} = \sum_{n=-\infty}^{+\infty}|h_{sr}(nT_s)|^2 \ / \ \sum_{n=-\infty}^{+\infty}|h_{sd}(nT_s)|^2$ and
$G_{rd} = \sum_{n=-\infty}^{+\infty}|h_{rd}(nT_s)|^2 \ / \ \sum_{n=-\infty}^{+\infty}|h_{sd}(nT_s)|^2$, where $h_{sr}(t)$ and $h_{rd}(t)$ are the electrical CIRs for S→R and R→D links, i.e., $h_{sr}(t) = p(t)\otimes c_{sr}(t)\otimes p(-t)$ and
$h_{rd}(t) = p(t)\otimes c_{rd}(t)\otimes p(-t)$.

Let $x_s(t)$ denote the transmitted signal from the source terminal with power $2EK_E$. Then, the electrical signals received by the destination and relay terminals in

the first phase can be written as

$$y_{D1}(t) = K_L L_T x_s(t) \otimes h_{sd}(t) + v_{D1}(t) \tag{9}$$

$$y_R(t) = K_L L_T \sqrt{G_{sr}} x_s(t) \otimes h_{sr}(t) + v_R(t) \tag{10}$$

where $v_{D1}(t)$ and $v_R(t)$ are the AWGN terms with zero mean and variance of σ_n^2.

In the AF mode, the relay terminal performs a simple scaling operation on the received signal. It is assumed that the amplification is performed in electrical domain where the relay node first removes the DC component in the received signal and then scales the power of the waveform to $2E(1 - K_E)$. Finally, the relay terminal adds a DC term to the information signal and modulates its LEDs. The scaling factor at the relay terminal in electrical domain is

$$G_A = \sqrt{\frac{2E(1 - K_E)}{2EK_E K_L^2 L_T^2 G_{sr} + \sigma_n^2}}. \tag{11}$$

The signal received by the destination terminal in the relaying phase can then be written as

$$y_{D2}(t) = (1 - K_L) L_T G_A \sqrt{G_{rd}} y_R(t) \otimes h_{rd}(t) + v_{D2}(t), \tag{12}$$

where $v_{D2}(t)$ is noise term added in the relay phase at the destination with zero mean and variance σ_n^2.

The destination performs maximal ratio combining (MRC) on the signals received over two phases as given by (9) and (12).

In the DF mode, the relay terminal first decodes the received signal in (10), re-modulates, and then forwards it to the destination. If $\hat{x}_s(t)$ denotes the emitted signal by the relay terminal with power $2E(1 - K_E)$, then the signal received by the destination terminal in the relaying phase can be written as

$$y_{D_2}(t) = (1 - K_L) L_T \sqrt{G_{rd}} \hat{x}_s(t) \otimes h_{rd}(t) + v_{D_2}(t). \tag{13}$$

The destination then performs MRC on the signals received over two phases given by (9) and (13).

CHAPTER IV

PERFORMANCE ANALYSIS AND OPTIMIZATION UNDER ILLUMINATION CONSTRAINTS

4.1 AF Relaying

The approximate BER for an OFDM system with square QAM constellations over AWGN channel is given as [26]

$$BER \approx \frac{2(\sqrt{M}-1)}{\sqrt{M}\log_2\sqrt{M}}\mathrm{Q}\left(\sqrt{\frac{3\mathrm{SNR}}{M-1}}\right) \tag{14}$$

where M is the modulation order and $Q(.)$ is the tail probability of the standard distribution. Using the Chernoff bound of Q function, (14) can be written as

$$BER \leq \frac{(\sqrt{M}-1)}{\sqrt{M}\log_2\sqrt{M}}\exp\left(-\frac{3\mathrm{SNR}}{2(M-1)}\right). \tag{15}$$

In cooperative transmission, the SNR at the output of MRC is the sum of individual SNRs in each cooperation phase [27]. Based on (9) and (12), SNRs in the S→D and S→R→D links can be written as

$$SNR_{sd} = \frac{2EK_EK_L^2L_T^2}{\sigma_n^2}, \tag{16}$$

$$SNR_{srd} = \frac{2EK_E(1-K_L)^2L_T^2G_A^2G_{rd}K_L^2L_T^2G_{sr}}{\sigma_n^2[(1-K_L)^2L_T^2G_A^2G_{rd}+1]} \tag{17}$$

Therefore, the SNR in the AF mode is

$$\begin{aligned} SNR_{AF} &= SNR_{sd} + SNR_{srd} \\ &= \frac{2EK_EK_L^2L_T^2}{\sigma_n^2} \\ &+ \frac{2EK_E(1-K_L)^2L_T^2G_A^2G_{rd}K_L^2L_T^2G_{sr}}{\sigma_n^2[(1-K_L)^2L_T^2G_A^2G_{rd}+1]} \\ &= 2\gamma K_E{K_L}^2 + \frac{2\gamma K_EK_L^2G_{sr}}{\frac{2\gamma K_EK_L^2G_{sr}+1}{2\gamma(1-K_E)(1-K_L)^2G_{rd}}+1}. \end{aligned} \tag{18}$$

In the following, the optimum power allocation (OPA) between the source and relay terminals is determined in order to minimize the BER of the cooperative system with RF relaying. Due to the negative exponential dependency, minimization of the BER in (14) is equivalent to the maximization of SNR in (18). Chapter II demonstrated that K_L gives control over the illumination performance. Since the primary task of lighting equipment is illumination, it is reasonable to fix K_L for a desired luminance ratio and determine the value of K_E to optimize the communication performance.

For a fixed K_L value, when (18) is differentiated with respect to K_E and equate it to zero,

$$K_E = \frac{A_0 A_1 - (1-K_L)\sqrt{A_0 A_1 G_{sr} G_{rd}(2\gamma K_L^2 G_{sr}+1)}}{2\gamma A_0[G_{rd}(1-K_L)^2 - G_{sr}K_L^2]} \tag{19}$$

where $A_0 = (G_{sr}+1)G_{rd}(1-K_L)^2 - K_L^2 G_{rd}$ and $A_1 = 1+2\gamma G_{rd}(1-K_L)^2$, is obtained.

As an example, consider Configuration A and the system parameters in Table 2 [28]. Based on the optical PDPs provided in Fig. 4, the geometric channel gains for S→R and R→D links are calculated as $G_{sr} = 7.98$ dB and $G_{rd} = 43.12$ dB. As earlier mentioned, the luminance ratio (L_R) of the task surface to the adjacent walls within the field of vision is recommended to be less than 5. When the L_R is set at 5, K_L becomes 0.92 which means 92% of the LEDs are employed at the ceiling and the rest at the task light. When the L_R is set at 3, K_L becomes 0.96.

Table 2: System Parameters

Number of subcarriers (N)	64
Number of guard band subcarrier (N_g)	4
Sampling interval (T_s)	50 nsec
Transmit pulse shaping filter ($p(t)$)	Truncated sinc pulse
LED Turn-on voltage (V_{tov})	2.75 V
LED max. allows voltage (V_{max})	4 V
DC Bias voltage (B)	3.37 V
Noise variance (σ_n^2)	0 dBm
Number of LEDs (L_T)	1

The pair of K_L values for each configuration which give the luminance ratios 3 and 5 are listed in Table 3. For both desk light and floor light configurations, it is seen that as the height of the task light increases, the number of allocated LED chips also increases in order to ensure the same L_R. For instance, Configuration A achieves the L_R of 5 with $K_L = 0.92$, whereas Configuration F achieves the same L_R with $K_L = 0.81$.

For fixed K_L values, Table 3 also lists the optimum K_E values obtained through numerical optimization of (18) for the information signal power range of 0-10 dBm. For example, consider Configuration A and assume 10 dBm. It is observed that the optimum K_E becomes 0.70 when $K_L = 0.96$. In other words, 70% of the AC power should be allocated to the source terminal for BER optimization while ensuring $L_R = 3$. For $K_L = 0.92$ (i.e., $L_R = 5$), the optimum value of K_E becomes 0.83, indicating that the source terminal should now consume 83% of the total AC power budget. It should be also noted that the closed form expression derived for optimum K_E in (19) gives perfect match with the values in Table 3.

As another benchmark, the joint optimization of K_E and K_L is determined based on (18) without any constraint in lighting performance. For example, in Configuration A, the joint optimization suggests that approximately 88% of LED chips are used at the source terminal, i.e., allocating 88% of the AC power to the source terminal, which is significantly higher than that found above under illumination constraints. In fact, for all six configurations under consideration, the optimum K_L values obtained without any lighting constraint violate the illumination requirements and give luminance ratios larger than 5. This supports the approach of fixing K_L first and optimizing only K_E for a given luminance ratio.

Table 3: Optimum K_L and K_E for relay assisted AF DCO-OFDM VLC

Signal Power (dBm)		No Lighting Constraint		$L_R = 3$		$L_R = 5$	
		K_L	K_E	K_L	K_E	K_L	K_E
0	A	0.8857	0.8857	0.9659	0.7993	0.9270	0.8281
	B	0.8335	0.8335	0.9610	0.5697	0.9172	0.7070
	C	0.7279	0.7279	0.9464	0.3878	0.8903	0.4942
	D	0.7351	0.7351	0.9306	0.4450	0.8587	0.5770
	E	0.7024	0.7023	0.9166	0.4376	0.8343	0.5477
	F	0.6678	0.6679	0.9077	0.4124	0.8183	0.5001
2	A	0.8865	0.8866	0.9659	0.7011	0.9270	0.8301
	B	0.8346	0.8346	0.9610	0.5674	0.9172	0.7088
	C	0.7286	0.7286	0.9464	0.3797	0.8903	0.4932
	D	0.7360	0.7361	0.9306	0.4392	0.8587	0.5773
	E	0.7033	0.7034	0.9166	0.4293	0.8343	0.5474
	F	0.6687	0.6687	0.9077	0.4016	0.8183	0.4988
4	A	0.8871	0.8871	0.9659	0.7022	0.9270	0.8314
	B	0.8353	0.8353	0.9610	0.5660	0.9172	0.7100
	C	0.7290	0.7291	0.9464	0.3744	0.8903	0.4926
	D	0.7366	0.7366	0.9306	0.4354	0.8587	0.5775
	E	0.7040	0.7039	0.9166	0.4239	0.8343	0.5471
	F	0.6692	0.6693	0.9077	0.3944	0.8183	0.4979
6	A	0.8874	0.8875	0.9659	0.7029	0.9270	0.8322
	B	0.8358	0.8357	0.9610	0.5651	0.9172	0.7108
	C	0.7293	0.7294	0.9464	0.3709	0.8903	0.4923
	D	0.7370	0.7370	0.9306	0.4330	0.8587	0.5776
	E	0.7044	0.7043	0.9166	0.4204	0.8343	0.5470
	F	0.6696	0.6696	0.9077	0.3898	0.8183	0.4974
8	A	0.8877	0.8877	0.9659	0.7029	0.9270	0.8322
	B	0.8361	0.8360	0.9610	0.5645	0.9172	0.7113
	C	0.7295	0.7295	0.9464	0.3687	0.8903	0.4920
	D	0.7372	0.7372	0.9306	0.4315	0.8587	0.5776
	E	0.7046	0.7046	0.9166	0.4182	0.8343	0.5469
	F	0.6698	0.6698	0.9077	0.3868	0.8183	0.4970
10	A	0.8878	0.8878	0.9659	0.7037	0.9270	0.8336
	B	0.8362	0.8363	0.9610	0.5641	0.9172	0.7116
	C	0.7296	0.7296	0.9464	0.3673	0.8903	0.4919
	D	0.7374	0.7374	0.9306	0.4305	0.8587	0.5777
	E	0.7048	0.7047	0.9166	0.4168	0.8343	0.5469
	F	0.6699	0.6700	0.9077	0.3849	0.8183	0.4968

4.2 DF Relaying

Similar to the AF relaying case, the SNR at the output of the MRC is the sum of individual SNR in each cooperation phase. The SNR in S→D link is given in (16) and to calculate SNR in the S→R→D link: First, individual SNRs for S→R and R→D links are written, using (9) and (13), as

$$SNR_{sr} = \frac{2EK_E K_L^2 L_T^2 G_{sr}}{\sigma_n^2}, \tag{20}$$

$$SNR_{rd} = \frac{2E(1-K_E)(1-K_L)^2 L_T^2 G_{rd}}{\sigma_n^2}. \tag{21}$$

Based on the approximation in (14), the SNR can be written as a function of BER as

$$\text{SNR} \approx f(\text{BER}) = \left(\text{Q}^{-1} \left(\frac{\text{BER}\sqrt{M} log_2 \sqrt{M}}{2(\sqrt{M}-1)} \right) \right)^2 \frac{M-1}{3}. \tag{22}$$

BER in the S→R→D link (BER_{srd}) can be written as [29]

$$BER_{srd} = (1 - BER_{sr})BER_{rd} + BER_{sr}(1 - BER_{rd}) \tag{23}$$

where BER_{sr} and BER_{rd} are the BERs in the S→R and R→D links, respectively. Using (23), SNR_{srd} can be expressed in terms of SNR_{sr} and SNR_{rd} as

$$\begin{aligned} SNR_{srd} &= f[(1 - f^{-1}(SNR_{sr}))f^{-1}(SNR_{rd}) \\ &+ f^{-1}(SNR_{sr})(1 - f^{-1}(SNR_{rd}))]. \end{aligned} \tag{24}$$

Based on (16) and (24),

$$\begin{aligned} SNR_{DF} &= SNR_{sd} + SNR_{srd} \\ &= SNR_{sd} + f[(1 - f^{-1}(SNR_{sr}))f^{-1}(SNR_{rd}) \\ &+ f^{-1}(SNR_{sr})(1 - f^{-1}(SNR_{rd}))]. \end{aligned} \tag{25}$$

Derivation of closed-form expressions for optimum K_E based on (25) appears to be mathematically intractable. To simplify the derivation, it is noted that the

SNR on S→R→D link cannot exceed the SNR on either of the links, which yields an upper bound for SNR_{srd}, i.e., $SNR_{srd} \leq \min\{SNR_{sr}, SNR_{rd}\}$. Furthermore, when $\min\{SNR_{sr}, SNR_{rd}\}$ is sufficiently high, SNR in S→R→D link provides a tight approximation to $\min\{SNR_{sr}, SNR_{rd}\}$ [28]. Therefore, for high signal power, the SNR at the output of MRC can be rewritten as

$$SNR_{DF} \approx SNR_{sd} + \min\{SNR_{sr}, SNR_{rd}\}. \tag{26}$$

It is interested in searching for a K_E which maximizes the SNR_{DF} particularly in the S→R→D link, since SNR in S→D link can be maximized at $K_E = 1$. Under the assumption of that SNR_{sd} is relatively lower than minimum of SNR_{sr} and SNR_{rd}, a K_E value that maximizes $\min\{SNR_{sr}, SNR_{rd}\}$ becomes the optimum K_E since SNR_{srd} is approximated with the minimum of SNR_{sr} and SNR_{rd} as seen in (26). Considering that SNR_{sr} in (20) is an increasing function of K_E and SNR_{rd} in (21) is a decreasing function of K_E, there exists a K_E value, for which (20) and (21) yield the same SNR. This value of K_E is the optimum since for the other values of K_E, either one of the SNR_{sr} and SNR_{rd} gets smaller than the other one and limits SNR_{srd}. Therefore, for a fixed K_L, the optimum K_E can be obtained as, by equating (20) to (21),

$$K_E = \frac{(1 - K_L)^2 G_{rd}}{(1 - K_L)^2 G_{rd} + K_L^2 G_{sr}}. \tag{27}$$

In Table 4, the optimum K_E obtained through numerical optimization of (26) is presented. The system parameters are kept the same as those in AF relaying (Table 2). For Configuration A, as an example, it can be observed from the Table 4 that optimum K_E takes values within the range of 0.67 and 0.78 when the L_R is set to 3. For $L_R = 5$, optimum K_E is larger than 0.86. It should be also noted that the derived closed form solution in (27) gives a good match to numerical optimization results when the available signal power is sufficiently large.

Table 4: Optimum K_L and K_E for relay assisted DF DCO-OFDM VLC

Signal Power (dBm)		No Lighting Constraint		$L_R = 3$		$L_R = 5$	
		K_L	K_E	K_L	K_E	K_L	K_E
0	A	0.9046	0.9047	0.9659	0.6759	0.9270	0.8598
	B	0.8473	0.8473	0.9610	0.5694	0.9172	0.6924
	C	0.7505	0.7506	0.9464	0.4428	0.8903	0.4793
	D	0.7480	0.7480	0.9306	0.4868	0.8587	0.5642
	E	0.7056	0.7057	0.9166	0.5092	0.8343	0.5345
	F	0.6682	0.6681	0.9077	0.5044	0.8183	0.4951
2	A	0.9138	0.9138	0.9659	0.7073	0.9270	0.8884
	B	0.8606	0.8605	0.9610	0.5442	0.9172	0.7265
	C	0.7623	0.7623	0.9464	0.3655	0.8903	0.4636
	D	0.7624	0.7625	0.9306	0.4263	0.8587	0.5720
	E	0.7212	0.7212	0.9166	0.4336	0.8343	0.5312
	F	0.6826	0.6825	0.9077	0.4144	0.8183	0.4764
4	A	0.9209	0.9209	0.9659	0.7348	0.9270	0.9094
	B	0.8706	0.8707	0.9610	0.5260	0.9172	0.7550
	C	0.7703	0.7703	0.9464	0.3017	0.8903	0.4510
	D	0.7726	0.7727	0.9306	0.3747	0.8587	0.5794
	E	0.7323	0.7323	0.9166	0.3697	0.8343	0.5295
	F	0.6927	0.6927	0.9077	0.3397	0.8183	0.4609
6	A	0.9261	0.9262	0.9659	0.7563	0.9270	0.9241
	B	0.8779	0.8779	0.9610	0.5123	0.9172	0.7769
	C	0.7755	0.7756	0.9464	0.2512	0.8903	0.4417
	D	0.7795	0.7795	0.9306	0.3326	0.8587	0.5853
	E	0.7398	0.7397	0.9166	0.3174	0.8343	0.5286
	F	0.6994	0.6995	0.9077	0.2797	0.8183	0.4489
8	A	0.9298	0.9298	0.9659	0.7718	0.9270	0.9341
	B	0.8829	0.8829	0.9610	0.5024	0.9172	0.7923
	C	0.7789	0.7788	0.9464	0.2133	0.8903	0.4353
	D	0.7839	0.7839	0.9306	0.3005	0.8587	0.5895
	E	0.7446	0.7446	0.9166	0.2770	0.8343	0.5281
	F	0.7038	0.7037	0.9077	0.2338	0.8183	0.4403
10	A	0.9323	0.9323	0.9659	0.7823	0.9270	0.9407
	B	0.8862	0.8862	0.9610	0.4956	0.9172	0.8027
	C	0.7810	0.7810	0.9464	0.1864	0.8903	0.4310
	D	0.7867	0.7868	0.9306	0.2776	0.8587	0.5923
	E	0.7476	0.7477	0.9166	0.2476	0.8343	0.5278
	F	0.7065	0.7064	0.9077	0.2004	0.8183	0.4345

The results for joint optimization of K_L and K_E are presentd under the assumption that no lighting constraint is considered. The joint optimization of K_L and K_E for DF mode yields that the task light operating in DF mode is brighter than the task light operating in AF mode. This can be observed from higher optimum K_L values in the DF mode for each configuration. However, for both DF and AF relaying, the

joint optimum settings violate the illumination requirements and are not of practical relevance.

CHAPTER V

OPTIMAL POWER ALLOCATION IN THE PRESENCE OF CLIPPING NOISE

In the previous chapter, it is assumed that amplitude levels of the emitted waveforms from the terminals remain within the dynamic range of the LEDs to ensure no clipping distortion. If the amplitude levels fall beyond the dynamic range, clipping noise is introduced.

The transmitted signals can experience clipping either at the source, relay, or in some cases at both terminals. For example, when the AC power at the source terminal is low (i.e., by allocating most of the power to the relay), clipping distortion may only be introduced at the relay terminal. Similarly, consuming most of the available AC power at the source terminal may cause distortion at the source terminal but not at the relay terminal. Depending on the power allocation, the signal can be clipped at the both terminals. In this chapter, the OPA problem in the presence of clipping noise is re-visited.

Considering the dynamic range of the LED, the output OFDM signal $\overline{x}(t)$ can be rewritten as

$$\overline{x}(t) = \begin{cases} V_{max}, & x(t) > V_{max} \\ x(t), & \text{else} \\ V_{tov}, & x(t) < V_{tov}. \end{cases} \tag{28}$$

For performance analysis in the presence of clipping noise, the instantaneous amplitude of a DCO-OFDM signal $x(t)$ can be modeled as a Gaussian random variable for a large number of subcarriers ($N > 10$). When the power of information waveform is assumed to be E, the probability that $x(t)$ takes a value of x is denoted by $f_x(x) \sim$

N(B,E). The clipping noise power can then be calculated as

$$\sigma_c^2 = \int_{V_{max}}^{\infty} (x - V_{max})^2 f_x(x) dx + \int_{-\infty}^{V_{tov}} (x - V_{tov})^2 f_x(x) dx. \tag{29}$$

In the following, the signal models are rewritten in order to take into account the effect of clipping. For the direct transmission, the received signal in (6) can be rewritten as, assuming rg is unity,

$$y(t) = \sum_{i=1}^{L_T} [x(t) + c(t)] \otimes h_{sd}(t) + v(t) \tag{30}$$

where $c(t)$ denotes the distortion noise term with power σ_c^2. Then, the effective SNR including the clipping noise becomes $E/(\sigma_c^2 + \sigma_n^2/L_T^2)$ [30].

5.1 AF Relaying

For relay-assisted transmission, (10) can be rewritten as

$$\begin{aligned} y_R(t) &= K_L L_T \sqrt{G_{sr}} x_s(t) \otimes h_{sr}(t) \\ &+ K_L L_T \sqrt{G_{sr}} c_S(t) \otimes h_{sr}(t) + v_R(t) \end{aligned} \tag{31}$$

where $c_S(t)$ is the clipping noise term introduced at the source terminal and the power of the signal $x_s(t)$ emitted from the source is $2EK_E$. The relay terminal scales the received signal power to $2E(1 - K_E)$ and the scaling factor in the electrical domain is

$$G_A = \sqrt{\frac{2E(1 - K_E)}{P_s K_L^2 L_T^2 G_{sr} + \sigma_n^2}} \tag{32}$$

where P_s is the average power of the clipped information signal emitted by the source terminal. This can be calculated as

$$\begin{aligned} P_s &= \int_{V_{tov}}^{V_{max}} (x_s - B)^2 f_{x_s}(x_s) dx_s \\ &+ \int_{V_{max}}^{\infty} (V_{max} - B)^2 f_{x_s}(x_s) dx_s \\ &+ \int_{-\infty}^{V_{tov}} (V_{tov} - B)^2 f_{x_s}(x_s) dx_s \end{aligned} \tag{33}$$

where $f_{x_s}(x_s)$ follows N(B, $2EKE$). The signals received by the destination terminal over the two cooperation phases then become

$$y_{D_1}(t) = K_L L_T x_s(t) \otimes h_{sd}(t) + K_L L_T c_S(t) \otimes h_{sd}(t) + v_{D_1}(t) \tag{34}$$

$$\begin{aligned} y_{D_2}(t) &= (1-K_L) L_T G_A \sqrt{G_{rd}}[\\ &\quad K_L L_T \sqrt{G_{sr}} x_s(t) \otimes h_{sr}(t) + v_R(t)] \otimes h_{rd}(t) \\ &+ (1-K_L) L_T \sqrt{G_{rd}} c_{FR}(t) \otimes h_{rd}(t) + v_{D_2} \end{aligned} \tag{35}$$

where $c_{FR}(t)$ is the forwarded clipping noise by the relay terminal with power $\sigma^2_{c_{FR}}$ which includes the clipping distortion introduced at the relay terminal $c_R(t)$ or already introduced at the source terminal $c_S(t)$. The power of the clipping distortion terms $\sigma^2_{c_S}$ and $\sigma^2_{c_R}$ are calculated using (29) with $f_{x_s}(x_s) \sim$ N(B, $2EKE$) and $f_{x_R}(x_R) \sim$ N(B,$2EK_EK_L^2L_T^2G_{sr}G_A^2$), respectively.

The propagating signal in the S→R→D link can be clipped at either or both of the source and relay terminals. Fig. 6 shows the scaled signal at the relay terminal considering the dynamic range of the LEDs. When the signal emitted from the source terminal is not distorted, but the relay terminal scales it to a level exceeding the dynamic range, the forwarded clipping noise includes only the clipping noise introduced at the relay terminal, i.e., $\sigma^2_{c_{FR}} = \sigma^2_{c_R}$ (see Fig. 6.a). When the emitted signal from the source terminal is already distorted, but the scaled signal at the relay terminal is not, as given in Fig. 6.b., the forwarded clipping noise is equal to the received and amplified version of the clipping noise introduced at the source terminal, i.e., $\sigma^2_{c_{FR}} = K_L^2 L_T^2 G_{sr} G_A^2 \sigma^2_{c_S}$. And finally, when the propagating information signal is subject to clipping at both source and relay terminals, as in Figs. 6.c and d, the power of forwarded clipping noise can be written as

$$\sigma^2_{c_{FR}} = \max\{K_L^2 L_T^2 G_{sr} G_A^2 \sigma^2_{c_S}, \sigma^2_{c_R}\}. \tag{36}$$

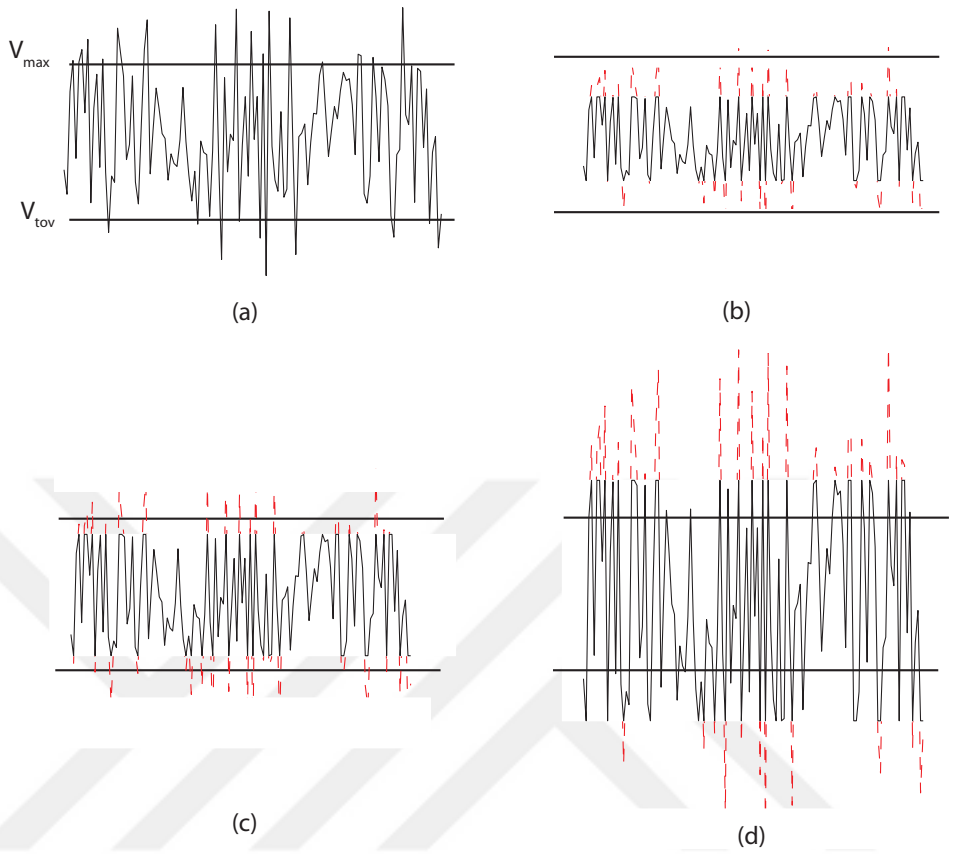

Figure 6: Illustration of the scaled signal at the relay terminal. The dashed lines are the amplitude levels already clipped at the source terminal. The signal is clipped (a) at the relay terminal only, (b) at the source terminal only, (c)-(d) at both terminals.

It should also be noted that once the signal is clipped at the source terminal, the clipping noise terms in both cooperation phases, become correlated. It is assumed that the receiver has the knowledge of clipping noise powers [29] and performs ideal noise whitening. Using (34) and (35), the SNR at the output of MRC can be expressed as

$$\begin{aligned} SNR_{AF} &= SNR_{sd} + SNR_{srd} \\ &= \frac{2EK_E K_L^2 L_T^2}{K_L^2 L_T^2 \sigma_{c_S^2} + \sigma_n^2} \\ &+ \frac{2EK_E K_L^2 L_T^2 G_A^2 G_{sr}}{\sigma_{c_{FR}^2} + \sigma_n^2 \frac{1+(1-K_L)^2 L_T^2 G_A^2 G_{rd}}{(1-K_L)^2 L_T^2 G_{rd}}}. \end{aligned} \tag{37}$$

Next, OPA is investigated to determine K_L and K_E values. Unlike the case of no clipping, a closed form expression for K_E is not available and numerical optimization of (37) is used. Table 5 tabulates the optimum K_L and K_E values for the relay-assisted VLC system in the presence of clipping noise. Due to the limited space, only the results for Configuration A are presented. Without lighting constraints and using high values of signal power, optimization of (37) suggests using nearly 100% of the LEDs at the source terminal and reducing the electrical signal power at the source terminal to maximize the SNR at the receiver. This is reasonable since any allocation of this high energy between the source and relay terminals will introduce clipping distortion at either or both of the terminals. Consequently, the optimum allocation suggests keeping the signal energy of the source terminal level with the maximum SNR. When the luminance ratio is set to 3 and 5, it is observed that the optimum K_E values again reduce the signal power at the source terminal. This is because the system performance is more sensitive to the clipping distortion at the source terminal since it affects the received signals in both cooperation phases.

Table 5: Optimum K_L and K_E for relay assisted AF DCO-OFDM VLC with clipping noise

Signal Power (dBm)	No Lighting Constraint		$L_R = 3$		$L_R = 5$	
	K_L	K_E	K_L	K_E	K_L	K_E
12	0.8887	0.8866	0.9659	0.7054	0.9270	0.8336
14	0.8990	0.8483	0.9659	0.6935	0.9270	0.8093
16	0.9321	0.6169	0.9659	0.5819	0.9270	0.6197
17	0.9414	0.5016	0.9659	0.5016	0.9270	0.5016
18	0.9445	0.5054	0.9659	0.5054	0.9270	0.5054
20	0.9581	0.5239	0.9659	0.5239	0.9270	0.5239
22	0.9910	0.2250	0.9659	0.2286	0.9270	0.2340
24	0.9958	0.1396	0.9659	0.1418	0.9270	0.1448
26	0.9974	0.0878	0.9659	0.0893	0.9270	0.0911
28	0.9982	0.0554	0.9659	0.0563	0.9270	0.0575
30	0.9987	0.0349	0.9659	0.0355	0.9270	0.0363

5.2 DF Relaying

In DF mode, the received signals by the relay and destination terminals in the broadcasting phase are the same as those in AF mode and are respectively given by (31) and (34). The relay terminal retrieves the source message signal, modulates and forwards the signal with power $2E(1-K_E)$. In the relaying phase, the received signal can be written as

$$\begin{aligned} y_{D_2}(t) &= (1-K_L)L_T\sqrt{G_{rd}}\hat{x}(t)\otimes h_{rd}(t) \\ &+ (1-K_L)L_T\sqrt{G_{rd}}c_r(t)\otimes h_{rd}(t) + v_{D_2}(t) \end{aligned} \tag{38}$$

where $c_s(t)$ and $c_r(t)$ are the introduced clipping noise terms respectively at the source and relay terminals and can be calculated using (29) with $f_{x_s}(x_s)$ as N(B, $2EKE$) and N(B, $2E(1-K_E)$). Based on (31), (34) and (38), individual SNRs for the S→D, S→R and R→D links in the presence of clipping noise are written as

$$SNR_{sd} = \frac{2EK_EK_L^2L_T^2}{\sigma_n^2 + K_L^2L_T^2\sigma_{c_S}^2}, \tag{39}$$

$$SNR_{sr} = \frac{2EK_EK_L^2L_T^2G_{sr}}{\sigma_n^2 + G_{sr}K_L^2L_T^2\sigma_{c_S}^2}, \tag{40}$$

$$SNR_{rd} = \frac{2E(1-K_E)(1-K_L)^2L_T^2G_rd}{\sigma_n^2 + G_{rd}(1-K_L)^2L_T^2\sigma_{c_R}^2}. \tag{41}$$

Finally, replacing (39), (40) and (41) in (26), SNR at the output of MRC for the DF mode can be written.

Table 6 lists the optimum K_L and K_E values for the relay-assisted DF VLC system in the presence of clipping noise obtained through numerical optimization for Configuration A. As in the AF mode, it is observed that, when the information signal power increases, OPA recommends consuming most of the AC power at the relay terminal in order to maintain high SNR in the S→D link. The optimum K_E values for high available information signal power are the same as in AF mode. This is because; in both AF and DF relaying, OPA maximizes the SNR in the S→D link which is independent of the relaying protocol.

Table 6: Optimum K_L and K_E for relay assisted DF DCO-OFDM VLC with clipping noise

Signal Power (dBm)	No Lighting Constraint		$L_R = 3$		$L_R = 5$	
	K_L	K_E	K_L	K_E	K_L	K_E
12	0.9350	0.9317	0.9659	0.7906	0.9270	0.9455
14	0.9517	0.8930	0.9659	0.8010	0.9270	0.9518
16	0.9789	0.6127	0.9659	0.6194	0.9270	0.6293
17	0.9806	0.4899	0.9659	0.4920	0.9270	0.4999
18	0.9647	0.4467	0.9659	0.4479	0.9270	0.4303
20	0.9618	0.4840	0.9659	0.4844	0.9270	0.4826
22	0.9916	0.2276	0.9659	0.2320	0.9270	0.2379
24	0.9956	0.1401	0.9659	0.1426	0.9270	0.1455
26	0.9973	0.0874	0.9659	0.0896	0.9270	0.0913
28	0.9981	0.0555	0.9659	0.0562	0.9270	0.0576
30	0.9987	0.0350	0.9659	0.0354	0.9270	0.0363

CHAPTER VI

ERROR RATE PERFORMANCE RESULTS

In this chapter, the BER performance of the proposed relay-assisted VLC system (with system parameters listed in Table 2) is presented. In order to make a fair comparison between cooperative and non-cooperative scenarios, it is assumed $2-$PSK for the direct transmission and $4-$PSK for the HD cooperative transmission that yield equal throughputs. Similarly, when $4-$PSK is used for the direct transmission, $16-$QAM is employed for the relay-assisted transmission.

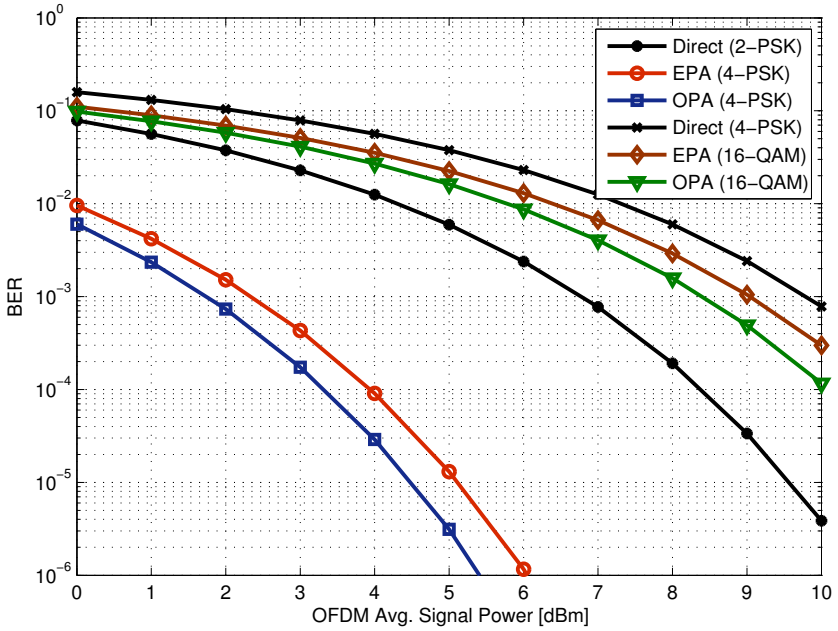

Figure 7: BER for AF relaying with EPA and OPA. Luminance ratio is 3 and Configuration A is considered.

In Figs. 7 and 8, the BER results for AF relaying with equal power allocation

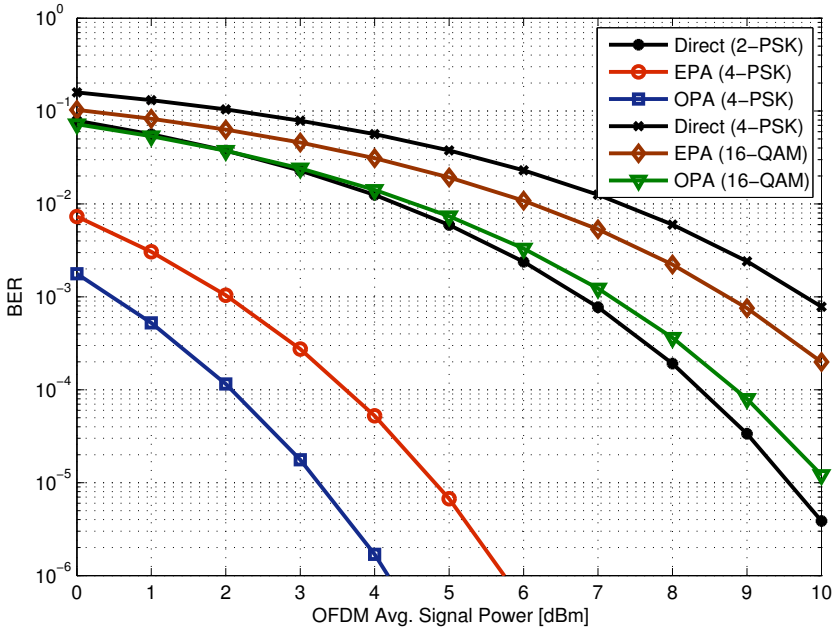

Figure 8: BER for AF relaying with EPA and OPA. Luminance ratio is 5 and Configuration A is considered.

(EPA) and OPA for Configuration A assuming L_R is 3 and 5, respectively, are presented. In EPA, it is assumed that the LED chips are distributed between the terminals according to a desired luminance ratio, but the signal power is equally shared. For OPA, corresponding values of K_E in Table 3 are used. In Fig. 7 , K_L is set to 0.96 under the assumption of $L_R = 3$. When $2-$ PSK and $4-$ PSK are considered respectively for the direct and cooperative transmissions, cooperative system with EPA provides a gain of 4.43 dB over direct transmission at a targeted BER value of 10^{-3}. For the same BER, this gain increases to 5.04 dB for OPA. When 4-PSK is considered for the direct transmission (16-QAM for the cooperative transmission), a cooperative system with EPA provides 0.75 dB gain with respect to direct transmission to achieve BER $= 10^{-3}$. With OPA, the performance gain is further improved to 1.38 dB.

In Fig. 8, luminance of the task surface is increased to the maximum recommended value of 5 (i.e., $K_L = 0.92$). When $2-$PSK and $4-$PSK are considered respectively for

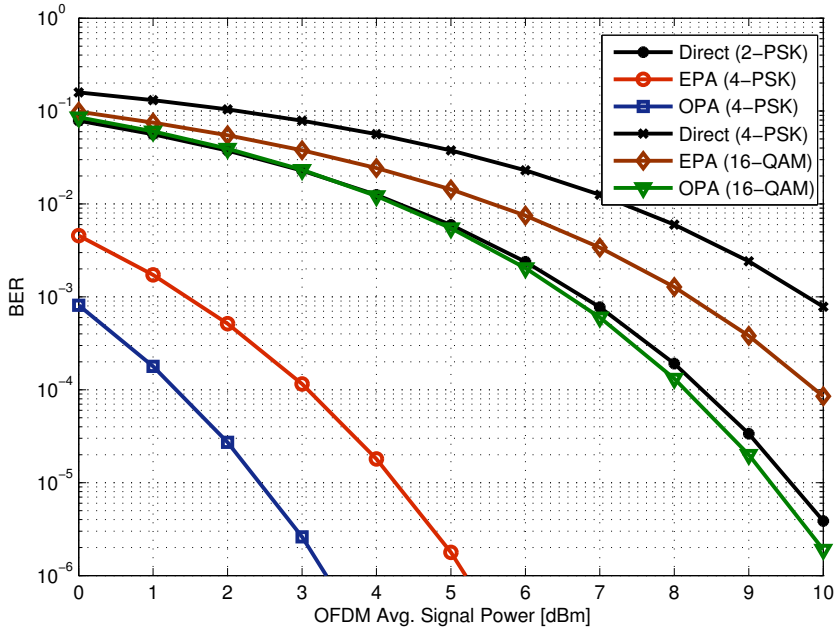

Figure 9: BER for DF relaying with EPA and OPA. Luminance ratio is 3 and Configuration A is considered.

the direct and cooperative transmission, the cooperative system with EPA achieves a gain of 4.75 dB over the direct transmission at BER $= 10^{-3}$ where OPA achieves 6.29 dB gain. When $4-\text{PSK}/16-\text{QAM}$ is considered for the direct/cooperative transmissions, the cooperative system with EPA has 1.04 dB gain whereas OPA achieves a gain of 2.61 dB. It is also observed that the performance of cooperative transmission is better when the L_R is set to 5, as compared to $L_R = 3$. This is because the distribution of AC and DC power between the terminals for $L_R = 5$ is close to the jointly optimum values.

In Figs. 9 and 10, the BER results for Configuration A assuming DF relaying is presented. In Fig. 9 (L_R is 3), when $2-\text{PSK}/4-\text{PSK}$ is considered for the direct/cooperative transmissions, 6.95 dB of SNR gain is achieved with OPA at BER of 10^{-3}. Whereas, when L_R is 5 (see Fig. 10), the gain is 7.58 dB. For both illumination levels, OPA provides considerable gain over the direct transmission and relay-assisted transmission with EPA. Similar to AF mode, when the relay operates in DF mode,

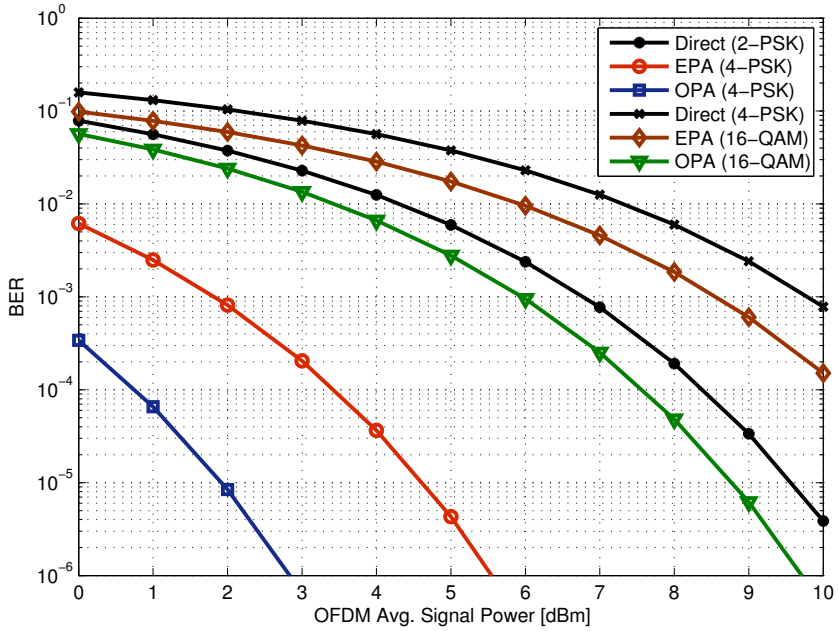

Figure 10: BER for DF relaying with EPA and OPA. Luminance ratio is 5 and Configuration A is considered.

the case of $L_R = 5$ gives better performance since the K_L and K_E values for L_R of 5 are close to joint optimum values.

Further comparison of performance results in Fig. 7 and Fig. 9 (for $L_R = 3$) shows that DF relaying outperforms the AF counterpart. Although the performance difference between AF and DF relaying is small for EPA, DF relaying is much better when OPA is used. Similarly, the comparison of the performance results in Fig. 8 and Fig. 10 (for $L_R = 5$) demonstrate that the performance gain is small with EPA for both AF and DF relaying. When OPA is employed, DF relaying provides more gain over AF.

In Figs. 11 and 12, the BER performances of all six configurations under consideration for AF relaying are compared. $4-$PSK and $16-$QAM are used for the direct and relay-assisted transmission, respectively. L_R is set at 5. In Fig. 11 where EPA is employed, it is observed that among the desk light configurations (i.e., A, B, C), Configuration B provides the least gain and Configuration C outperforms the other

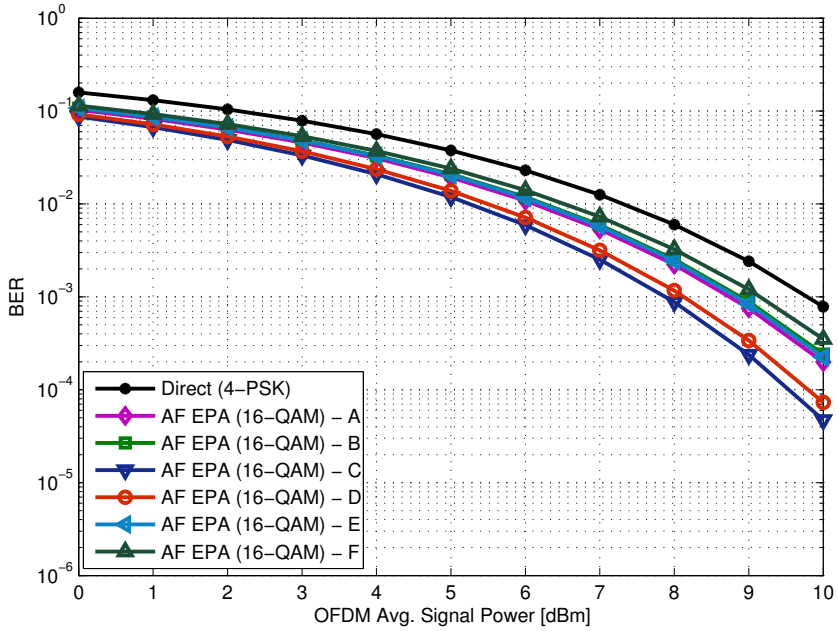

Figure 11: Comparison of BER for different configurations with EPA. Luminance ratio is 5 and AF relaying is assumed.

configurations. Specifically, to achieve a targeted BER $= 10^{-3}$, average signal power of 7.88 dBm is required in Configuration C indicating 1.9 dB gain over direct transmission. Note that the system performance depends not only the relative channel gains G_{sr} and G_{rd} (therefore not only the distances between the terminals) but also, K_L and K_E values. Therefore, a configuration which yields the maximum SNR would outperform the others. In the case, Configuration C is expected to yield the best performance among the three configurations under consideration since it yields the highest SNR based on (18). Similarly, among the floor light configurations, Configuration D gives the best performance and outperforms direct transmission by 1.65 dB. In Fig. 12, the performances of the configurations under the assumption of OPA are compared. It is observed that performance improvements through OPA with respect to EPA is limited for configurations C, D, E and F, since for these configurations, the optimum K_E values are already close to 0.5 as in EPA setting (Table 3). For Configurations A and B, on the other hand, improvements through OPA are more

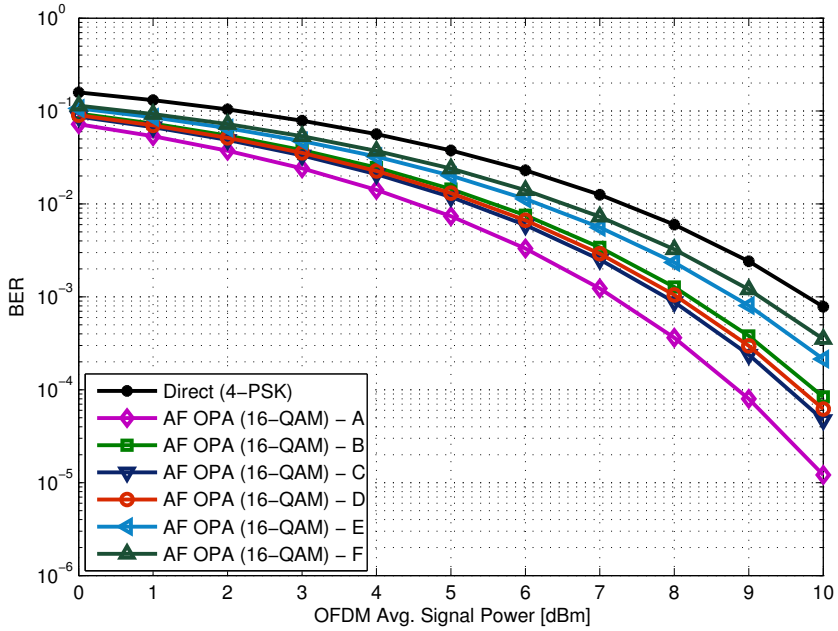

Figure 12: Comparison of BER for different configurations with OPA. Luminance ratio is 5 and AF relaying is assumed.

pronounced and performance gains of 2.61 dB and 2.07 dB are observed respectively with respect to direct transmission.

In Figs. 13 and 14, the BER performances for six configurations with DF relaying for EPA and OPA, respectively, are depicted. In case of EPA (Fig. 14), the configuration C which gives the highest SNR in (26) outperforms the others. Specifically, it achieves 3.98 dB gain with respect to the direct transmission. When OPA is employed (Fig. 14), similar to AF mode, the performance improvement is limited for configurations C, D, E and F since the optimum K_E values for these configurations are already close to 0.5 (Table 4). For configurations A and B, performance can be further improved with OPA, however, the best performance is still achieved with Configuration C which provides 4.12 dB performance gain with respect to direct transmission.

In Figs. 15 and 16, the BER performances of the cooperative transmission and the direct transmission in the presence of clipping distortion respectively for $L_R = 3$ and 5 are compared. Configuration A is considered. In order to observe the effect

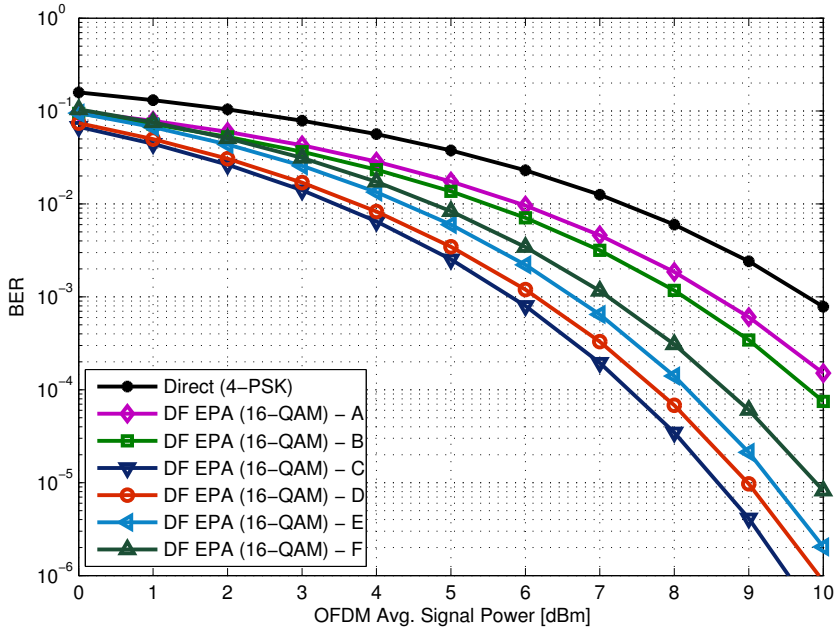

Figure 13: Comparison of BER for different configurations with EPA. Luminance ratio is 5 and DF relaying is assumed.

of clipping, the signal power levels are increased beyond 10 dBm. Note that the BER plots for signal power levels less than 10 dBm in these figures coincide with those in Figs. 7, 8, 9 and 10,. Optimum K_L and K_E values are chosen according to Tables 3 and 5 for AF protocol and Tables 4 and 6 for the DF protocol. The BER performance of cooperative transmission starts to degrade after the average signal power of approximately 17 dBm. At this signal power level, it can be observed from Tables 5 and 6 that OPA suggests sharing the available power equally for each cooperation phase and effectively reduces to EPA. Both AF and DF relaying (with either EPA or OPA) give very close performance when the available signal power is around 17 dBm. The reason is that the OPA rule recommends to decrease K_E as the available signal power grows (i.e., allocates most of the available AC power to the relay terminal) and when $K_E \leq 0.5$, distortion on the R→D link starts to increase where the SNR in S→D link is kept at the maximum level which is the same for both AF and DF protocols.

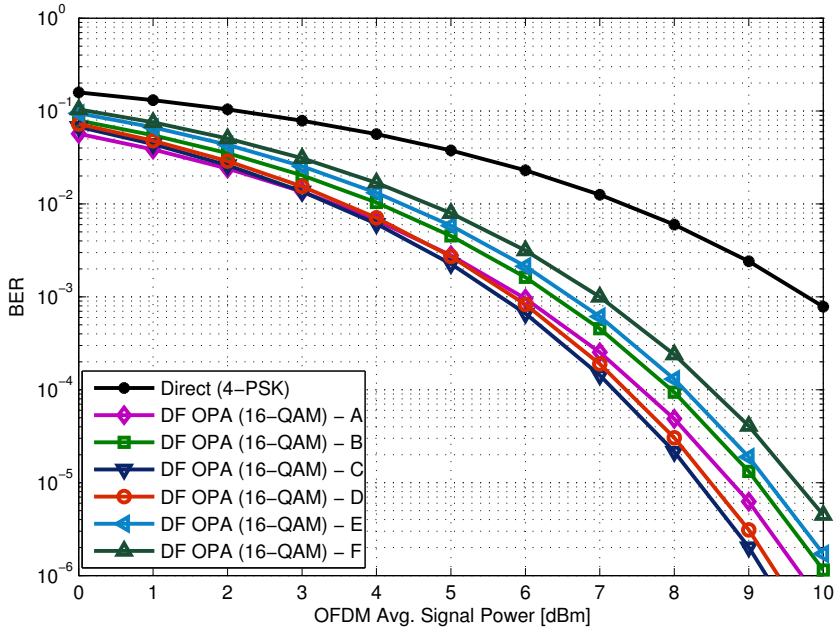

Figure 14: Comparison of BER for different configurations with OPA. Luminance ratio is 5 and DF relaying is assumed.

When the available OFDM signal power per cooperation phase is further increased (> 24 dBm), cooperative transmission with OPA again outperforms the direct transmission. In this region, as observed from Tables 5 and 6, OPA chooses to keep the signal level at the source terminal with less distortion and consumes most of the signal power at the relay terminal. This behavior yields saturation in the BER curve since maximum SNR is maintained in the broadcasting phase and high distortion noise is received in the relaying phase. This applies to both AF and DF protocols since in the broadcasting phase they achieve the same SNR.

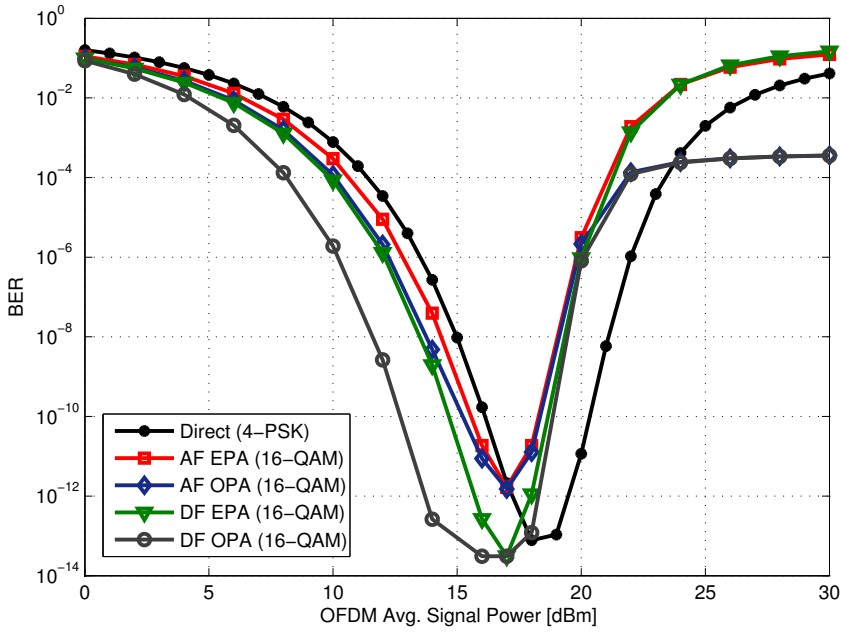

Figure 15: BER for relay-assisted VLC systems with clipping distortion. Luminance ratio is 3. Configuration A.

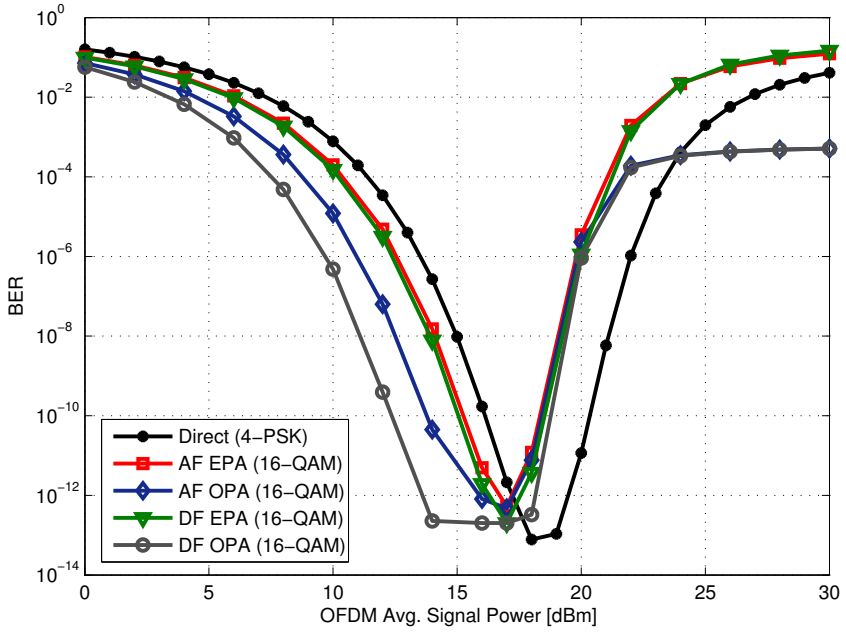

Figure 16: BER for relay-assisted VLC systems with clipping distortion. Luminance ratio is 5. Configuration A.

CHAPTER VII

CONCLUSION

The benefits of using a relaying terminal in an OFDM based VLC system are explored. An office space with an ambient light source (source terminal) and a task light (relay terminal) is considered. Under the assumption of HD relaying, the BER performance of the relay-assisted DCO-OFDM VLC system with either AF or DF relaying is evaluated and the performance is optimized through power allocation between the source and relay terminals under illumination constraints. Since the primary task of lightning equipment is illumination, the optimum allocation of available LED chips (i.e., which corresponds to DC power allocation) between the two light sources is determined to satisfy a desired luminance ratio. Then, the BER is minimized through AC power allocation. The results have shown that significant performance gains (depending on the modulation type and topology) can be obtained via cooperation compared to direct transmission. In addition, DF relaying provides higher gain over AF relaying with and without lighting constraints. Moreover, the effect of clipping noise is discussed and the cases when either direct or cooperative transmission is preferred are demonstrated.

Bibliography

[1] S. Arnon, J. Barry, G. Karagiannidis, R. Schober, and M. Uysal, *Advanced optical wireless communication systems*. Cambridge university press, 2012.

[2] T. Komine and M. Nakagawa, "Fundamental analysis for visible-light communication system using LED lights," *IEEE Transactions on Consumer Electronics*, vol. 50, pp. 100–107, Feb 2004.

[3] J. Armstrong, "OFDM for Optical Communications," *Journal of Lightwave Technology*, vol. 27, pp. 189–204, Feb 2009.

[4] J. Armstrong and A. J. Lowery, "Power efficient optical OFDM," *Electronics Letters*, vol. 42, pp. 370–372, March 2006.

[5] N. Fernando, Y. Hong, and E. Viterbo, "Flip-OFDM for Unipolar Communication Systems," *IEEE Transactions on Communications*, vol. 60, pp. 3726–3733, December 2012.

[6] A. H. Azhar, T. A. Tran, and D. O'Brien, "A Gigabit/s Indoor Wireless Transmission Using MIMO-OFDM Visible-Light Communications," *IEEE Photonics Technology Letters*, vol. 25, pp. 171–174, Jan 2013.

[7] S. D. Dissanayake and J. Armstrong, "Comparison of ACO-OFDM, DCO-OFDM and ADO-OFDM in IM/DD Systems," *Journal of Lightwave Technology*, vol. 31, pp. 1063–1072, April 2013.

[8] S. Dimitrov and H. Haas, "Information Rate of OFDM-Based Optical Wireless Communication Systems With Nonlinear Distortion," *Journal of Lightwave Technology*, vol. 31, pp. 918–929, March 2013.

[9] M. Zhang and Z. Zhang, "An Optimum DC-Biasing for DCO-OFDM System," *IEEE Communications Letters*, vol. 18, pp. 1351–1354, Aug 2014.

[10] H. Zhang, Y. Yuan, and W. Xu, "PAPR Reduction for DCO-OFDM Visible Light Communications via Semidefinite Relaxation," *IEEE Photonics Technology Letters*, vol. 26, pp. 1718–1721, Sept 2014.

[11] N. O. Tippenhauer, D. Giustiniano, and S. Mangold, "Toys communicating with LEDs: Enabling toy cars interaction," in *2012 IEEE Consumer Communications and Networking Conference (CCNC)*, pp. 48–49, Jan 2012.

[12] Z. Wu, *Free space optical networking with visible light: A multi-hop multi-access solution*. PhD thesis, Citeseer, 2012.

[13] S. Jo, B. An, *et al.*, "VLC Based Multi-hop Audio Data Transmission System," in *Grid and Pervasive Computing*, pp. 880–885, Springer, 2013.

[14] C. B. Liu, B. Sadeghi, and E. W. Knightly, "Enabling vehicular visible light communication (V2LC) networks," in *Proceedings of the Eighth ACM international workshop on Vehicular inter-networking*, pp. 41–50, ACM, 2011.

[15] H. Yang and A. Pandharipande, "Full-duplex relay VLC in LED lighting linear system topology," in *Industrial Electronics Society, IECON 2013 - 39th Annual Conference of the IEEE*, pp. 6075–6080, Nov 2013.

[16] H. Yang and A. Pandharipande, "Full-duplex relay VLC in LED lighting triangular system topology," in *Communications, Control and Signal Processing (ISCCSP), 2014 6th International Symposium on*, pp. 85–88, May 2014.

[17] H. Chowdhury and M. Katz, "Cooperative multihop connectivity performance in visible light communications," in *Wireless Days (WD), 2013 IFIP*, pp. 1–4, Nov 2013.

[18] G. R. Newsham and D. M. Sander, "The Effect of office design on workstation lighting: a simulation study," *Journal of the Illuminating Engineering Society*, vol. 32, no. 2, pp. 52–73, 2003.

[19] E. 12464-1:2011, "Light and lighting - Lighting of work places art 1: Indoor work places, ," *00169042*, 2011.

[20] J. R. Barry, J. M. Kahn, W. J. Krause, E. A. Lee, and D. G. Messerschmitt, "Simulation of multipath impulse response for indoor wireless optical channels," *IEEE Journal on Selected Areas in Communications*, vol. 11, pp. 367–379, Apr 1993.

[21] F. Miramirkhani, M. Uysal, and E. Panayirci, "Novel channel models for visible light communications," in *SPIE OPTO*, pp. 93870Q–93870Q, International Society for Optics and Photonics, 2015.

[22] E. F. Schubert, T. Gessmann, and J. K. Kim, *Light emitting diodes*. Wiley Online Library, 2005.

[23] E. Sarbazi, M. Uysal, M. Abdallah, and K. Qaraqe, "Indoor channel modelling and characterization for visible light communications," in *2014 16th International Conference on Transparent Optical Networks (ICTON)*, pp. 1–4, July 2014.

[24] E. Sarbazi, M. Uysal, M. Abdallah, and K. Qaraqe, "Ray tracing based channel modeling for visible light communications," in *2014 22nd Signal Processing and Communications Applications Conference (SIU)*, pp. 702–705, April 2014.

[25] J. N. Laneman, D. N. C. Tse, and G. W. Wornell, "Cooperative diversity in wireless networks: Efficient protocols and outage behavior," *IEEE Transactions on Information Theory*, vol. 50, pp. 3062–3080, Dec 2004.

[26] K. Cho and D. Yoon, "On the general BER expression of one- and two-dimensional amplitude modulations," *IEEE Transactions on Communications*, vol. 50, pp. 1074–1080, Jul 2002.

[27] D. Brennan, "Linear diversity combining techniques," *Proceedings of the IRE*, vol. 47, no. 6, pp. 1075–1102, 1959.

[28] T. Wang, A. Cano, G. B. Giannakis, and J. N. Laneman, "High-Performance Cooperative Demodulation With Decode-and-Forward Relays," *IEEE Transactions on Communications*, vol. 55, pp. 830–830, April 2007.

[29] E. Bjornson, M. Matthaiou, and M. Debbah, "A New Look at Dual-Hop Relaying: Performance Limits with Hardware Impairments," *IEEE Transactions on Communications*, vol. 61, pp. 4512–4525, November 2013.

[30] R. Mesleh, H. Elgala, and H. Haas, "On the Performance of Different OFDM Based Optical Wireless Communication Systems," *IEEE/OSA Journal of Optical Communications and Networking*, vol. 3, pp. 620–628, August 2011.